Adsorption and Dissociation of CO on Bare and Ni-Decorated Stepped Rh (553) Surfaces

ARTICLE *in* THE JOURNAL OF PHYSICAL CHEMISTRY C · JANUARY 2009

Impact Factor: 4.77 · DOI: 10.1021/jp806424t

Article

Adsorption and Dissociation of CO on Bare and Ni-Decorated Stepped Rh(553) Surfaces

A. Stroppa, F. Mittendorfer, J. N. Andersen, G. Parteder, F. Allegretti, S. Surnev, and F. P. Netzer

J. Phys. Chem. C, **2009**, 113 (3), 942-949 • Publication Date (Web): 30 December 2008

Adsorption and Dissociation of CO on Bare and Ni-Decorated Stepped Rh(553) Surfaces

A. Stroppa,[†] F. Mittendorfer,*[,†] J. N. Andersen,[‡] G. Parteder,[§] F. Allegretti,[§] S. Surnev,[§] and F. P. Netzer[§]

Faculty of Physics and Centre for Computational Materials Science, Universität Wien, A-1090 Wien, Austria, Institute of Synchrotron Radiation Physics, Lund University, S-221 00 Lund, Sweden, and Institute of Physics, Surface and Interface Physics, Karl-Franzens University Graz, A-8010 Graz, Austria

Received: July 21, 2008; Revised Manuscript Received: November 1, 2008

The adsorption and dissociation of carbon monoxide were studied with plane-wave density functional theory on flat Rh(111), stepped and kinked Rh(553), and Ni-decorated Rh(553) surfaces. The theoretical results were compared to high-resolution X-ray photoelectron spectroscopy (HR-XPS) experiments. The most favorable CO adsorption sites for low coverages were identified by a systematic calculation of the adsorption energies, and their sequence of occupation as a function of CO exposure was determined experimentally in C 1s HR-XPS spectra via their characteristic surface core-level shifts. On the clean, stepped (553) surface, molecular CO is adsorbed more strongly on low-coordinated top sites at the step edge, but on the Ni-decorated surface, the binding is stronger at the terrace sites. The barrier for dissociation with respect to the gas phase is about 1 eV lower on the stepped Rh(553) surface than on the flat Rh(111) surface, implying a substantially higher reaction rate. The presence of kinks at the clean Rh(553) surface does not lead to a significant additional decrease of the dissociation barriers, resulting in dissociation energies just above the desorption threshold for both stepped and kinked surfaces, whereas the barrier can be additionally lowered by about 0.1 eV by decorating the step edges with Ni stripes. Whereas no dissociation of CO was observed by HR-XPS on the clean Rh(553) surface, a minor amount of CO dissociation was found on the Ni-decorated Rh surface, in agreement with the theoretical predictions.

1. Introduction

The study of the interaction of carbon monoxide with transition metal surfaces (the first step to oxidation of CO with oxygen on a metal surface) has been of great interest for several decades,[1−6] both for the relevant technological applications in, for instance, the catalytic oxidation of CO in automotive exhaust purification catalysts and as a prototype reactant in studies aiming to provide an understanding of catalytic reactions in general.[3,7,8] A great amount of experimental data has been obtained for CO adsorption on metals, including binding energies (via thermal desorption spectroscopy or microcalorimetry), electronic structure (via photoemission spectroscopy), vibrational frequencies (via high-resolution electron energy loss or infrared spectroscopies), and preferred adsorption sites (via, e.g., low-energy electron diffraction). In many cases, a microscopic interpretation of the experimental results benefits from state-of-the-art simulations. In this respect, the adsorption of carbon monoxide on flat rhodium surfaces has been investigated in great detail, both experimentally and theoretically.[9−16] Rhodium is one of the most versatile catalysts. It is employed to reduce nitrogen and carbon monoxide in the exhaust of internal combustion engines and shows particular behavior in catalysis involving CO.[17−19] Obviously, the chemisorption behavior of CO on rhodium is the primary step to understand the mechanism of catalytic processes involving CO, such as methanation, Fischer−Tropsch synthesis, the formation of alcohols, and the CO oxidation reaction.

In the past several years, attention has turned from low-Miller-index surfaces to those with defects such as steps and kinks. Undoubtedly, stepped surfaces have acquired great attention for a number of reasons. Steps at surfaces provide favorable sites for chemical reactions and nucleation,[20] basically because of the observed enhanced reactivity of the stepped surfaces.[21−24] As a result of the variety of local environments of the surface atoms, vicinal surfaces provide a ready-made atomic laboratory for examining the effects of local coordination and geometry on system characteristics. The role of steps in chemical reactions such as molecular dissociation has been the subject of intense recent scientific attention [6,25,26] Last, but not least, because step edges act as preferred nucleation sites and because the activation barrier for diffusion of adatoms along the steps is often lower than that of adatoms on a flat terrace, low-dimensional nanostructures of good quality are obtained by atom deposition on stepped substrates as templates.[27−29]

Detailed theoretical[30−32] and experimental data are available for CO dissociation on flat[33] and stepped[34,35] surfaces, as well as on small Rh particles of varying size.[36−38] In a previous work, we focused on a theoretical and experimental study of the adsorption and vibrational properties of CO on stepped Rh(553).[39] In this work, we focus on the adsorption and dissociation of CO on bare and Ni-decorated stepped Rh(553) surfaces, which has not been investigated yet by ab initio calculations, and compare the results with experimental core-level spectra obtained from high-resolution XPS measurements.

This article is organized as follows: In section 2, we describe the computational and experimental details. In section 3, we study the adsorption and dissociation of CO on the bare stepped and kinked Rh(553) surface and compare them with the flat Rh(111) surface. In section 4, we address the CO adsorption

* Corresponding author. E-mail: florian.mittendorfer@univie.ac.at.
[†] Universität Wien.
[‡] Lund University.
[§] Karl-Franzens University Graz.

10.1021/jp806424t CCC: $40.75
Published on Web 12/30/2008

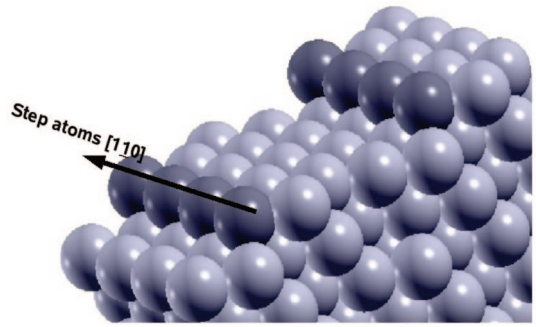

Figure 1. Perspective and top view of the clean Rh(553) stepped surface. Dark gray spheres represent step atoms. Light gray spheres represent terrace atoms. The arrow indicates the direction of the monatomic step row.

and dissociation on nickel-decorated Rh(553), and in section 5, we provide a summary.

2. Computational and Experimental Details

Our calculations were performed with the Vienna ab initio simulation package (VASP)[40,41] using the generalized gradient approximation (GGA) to DFT in the Perdew−Burke−Ernzerhof parametrization for the exchange-correlation energy functional.[42] In addition, selected sites were investigated using the HSE03 hybrid Hartree−Fock functional. [43]

The interaction between the ions and valence electrons was described by the projector augmented wave (PAW)[44] method in the implementation of Kresse and Joubert.[45] The Rh(553) surface consisted of five-atom-wide (111) terraces separated by monatomic 111-faceted steps approximately 10 Å apart. Figure 1 shows a schematic drawing of the perspective view of the supercell used to simulate the Rh(553) surface. Full details of the computational setup are given in ref 39. The free CO molecule was characterized by a calculated equilibrium bond length of 1.143 Å, in good agreement with the experimental value of 1.128 Å.[46]

The transition states (TSs) of the reactions were obtained by combining the nudged elastic band (NEB) method of Jonsson et al.[47−49] with the improved dimer method,[50] which was recently implemented in the VASP code. This method, initially developed by Henkelman and Jónsson,[51] is a local saddle-point search algorithm that uses only first derivatives of the potential energy. For details, we refer to the literature.[51] The starting configuration for the improved dimer method was extracted from a previous NEB calculation by considering an interpolated position between the two uppermost images having opposite tangential forces along the reaction path. The transition states were verified by calculating the vibrational spectra. The core-level shifts (CLSs) were evaluated including final state contributions as described in ref 52.

Extensive tests[32] have shown that the numerical accuracy of the adsorption energies is about 20 meV within the chosen exchange-correlation functional. In addition, GGA functionals tend to overestimate total adsorption energies by up to 150 meV. Nevertheless, the relative errors for the comparison of different adsorption sites tend to be much smaller. The NEB calculations in combination with the improved dimer method and a verification of the vibrational spectrum allow for the determination of the transition state within a numerical accuracy of 50−100 meV. Finally, for the core-level shifts, the expected accuracy is 20−50 meV.[52]

High-resolution X-ray photoelectron spectra were recorded at beamline I311 at the Swedish synchrotron radiation laboratory

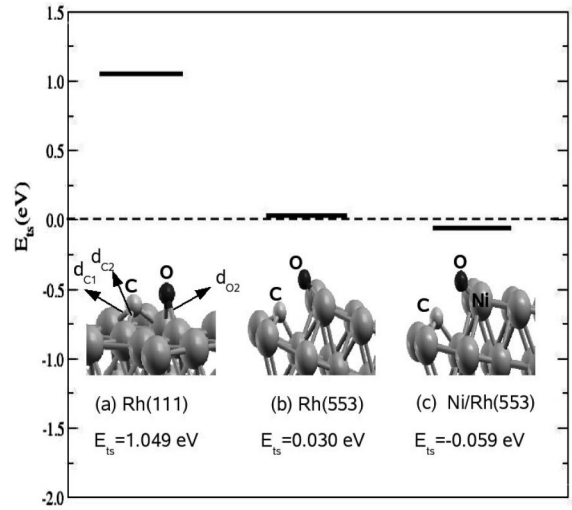

Figure 2. Energy barriers and perspective view of the TS geometries for CO dissociation on (a) the clean flat Rh(111) surface, (b) the clean Rh(553) surface, and (c) the nickel-decorated Rh(553) surface. Pale-gray spheres are Rh atoms; C, O, and Ni atoms are explicitly labeled. The carbon−metal (d_{C1}, d_{C2}) and oxygen−metal (d_{O2}) distances are directly shown in the figure for the flat surface. (d_{C3} and d_{O1} are not shown for clarity but are easily found by inspection of the figure). The same notation holds for parts b and c.

MAX-Laboratory, Lund, Sweden; the beamline and the electron spectrometer end station have been specified previously.[53] The total energy resolution employed in the present experiments was ∼100 meV. The vicinal Rh(553) surface was cleaned by being heated in oxygen and subjected to cycles of Ar ion bombardment and annealing. Nickel adatoms were deposited by physical vapor deposition from an electron beam evaporator; a typical evaporation rate was 0.1 monolayer (ML)/min as measured by a quartz microbalance. Deposition of 0.2 ML of Ni onto Rh(553) at 420 K resulted in a regular decoration of all Rh step edges by monatomic Ni rows, as reported previously.[29] Carbon monoxide was dosed via a leak valve from the system ambient; exposures are given in Langmuir (1 L = 1 × 10^{-6} Torr s).

3. CO Dissociation on Rh(111) and Rh(553)

In a previous study,[39] we showed that the adsorption on stepped surfaces is, in general, stronger than on flat surfaces, especially for low-coordinated sites. Here, we present a detailed study of the adsorption and dissociation of CO on the stepped Rh(553) surface and on a Rh(553) surface that contains kinks at the step edges, as well as some results for the flat Rh(111) surface for comparison.

3.1. Flat Rh(111) Surface. The dissociation of CO on the flat Rh(111) surface has been investigated in several theoretical studies.[54,55] Yet, we have repeated these calculations here to provide a consistent comparison for our results on the Rh(553) surfaces.

Figure 2a illustrates the geometries at the transition state. In the transition state (TS) complex, the C atom is near the hexagonal close-packed (hcp) hollow site, and the O atom is in the bridge site close to it. Four surface atoms are directly involved in bonding with the TS complex, with one of the surface atoms being shared by both C and O (see Figure 2a). For the sake of comparison, we report our results in terms of the intrinsic (apparent) reaction barrier (E_{ts}), that is, the adsorption energy of the TS with respect to the gas phase. Positive values of the intrinsic reaction barrier indicate that the energy barrier for the dissociation is higher than the barrier for

TABLE 1: Structural Parameters, Apparent Dissociation Barriers (E_{ts}), and Absolute Barriers with Respect to the Adsorbed CO Molecule (E_{barr}) of the Transition States for CO Dissociations on Rh(111), Rh(553), and Nickel-Decorated Rh(553) Surfaces[a]

surface	d_{C1} (Å)	d_{C2} (Å)	d_{C3} (Å)	d_{O1} (Å)	d_{O2} (Å)	d_{CO} (Å)	E_{ts} (eV)	E_{barr} (eV)
Rh(111)	1.964	1.880	1.959	2.055	2.005	1.897	1.05	3.02
Rh(111)[54]	1.921	1.909	1.954	2.094	2.066	1.897	1.25	−
Rh(553)	1.922	1.919	1.974	1.970	1.967	2.033	0.03	2.08
Ni/Rh(553)	1.910	1.908	1.966	1.819	1.819	2.084	−0.06	2.06

[a] d_{C1}, d_{C2}, d_{C3}, d_{O1}, and d_{O2} are labeled in Figure 2. d_{CO} is the CO bond length.

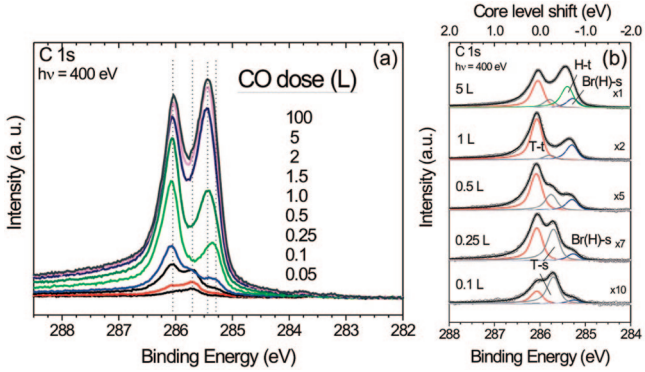

Figure 3. (a) C 1s core-level spectra of the Rh(553) surface exposed to various amounts of CO at 90 K (in langmuir, L). Dotted lines are guides to the eye to emphasize different spectral components. (b) Quantitative decomposition analysis of selected C 1s spectra into different spectral components. For labeling, see text.

molecular desorption. In Table 1, we report the main geometrical parameters as well as the apparent reaction barriers. For the definition of the distances, see Figure 2a. We found that the transition state has a long stretched distance between C and O (late transition state, $d_{CO} = 1.964$ Å) and leads to a calculated intrinsic energy barrier of 1.05 eV. Our results differ slightly from the study of ref 54: Although the geometry of TS is the same, the atomic distances differ by up to 0.05 Å, and the E_{ts} values differ up to 0.2 eV. In ref 55, E_{ts} is 1.53 eV, which differs by about 0.3 eV from our value. This is most likely due to the use of different computational parameters.[54,55]

3.2. Rh(553) Stepped Surface. The Rh(553) surface is a stepped surface consisting of terraces with the (111) orientation and monatomic steps with (111) microfacets. Before considering the dissociation of CO, it is of interest to examine how the different adsorption sites at step edges and at the terraces become populated by CO as a function of CO exposure and coverage. The low-coverage adsorption of CO on Rh(553) was studied with ab initio approaches in a previous publication to which we refer for further discussion.[39] The calculations show only a minor increase in the adsorption energy in the vicinity of the step edge (see Table 3). In addition, the adsorption energy in the undercoordinated top site at the step edge is underestimated using standard (GGA) DFT, and the correct site preference for low-coverage adsorption—the top site at the step edge—can be restored only by using post-DFT approaches such as the HSE03 hybrid functional.[39] Therefore, an additional experimental confirmation is highly desirable. High-resolution C 1s core-level spectra of CO are well-suited to tackle this problem experimentally, because the various adsorption sites are distinguished by characteristic surface core-level shifts (SCLSs).

Figure 3a shows a set of C 1s core-level spectra of CO adsorbed on Rh(553) at 90 K as a function of CO exposure. It is clear that the spectra contain a number of different components (dashed lines) that vary in intensity as a function of CO exposure. Figure 3b displays a selection of spectra that have been subjected to a careful decomposition analysis following well-established procedures.[56] The top horizontal axis represents the C 1s surface core-level shift (SCLS) scale with respect to the binding energy of 286.00 eV of the T-t component. For high CO exposures (>2 L), the spectra are dominated by two spectral components at binding energies (BEs) of 286.00 eV (T-t) and 285.38 eV (H-t) that can be assigned to the emission from CO molecules adsorbed on the terraces in on-top sites (T-t) and three-fold hollow sites (H-t), respectively. This is in close analogy to the C 1s spectra from CO on the flat Rh(111) surface, as reported and analyzed by Beutler et al.[57] Our own SCLS calculations also indicate that CO molecules adsorbed in on-top sites on Rh(111) and on the (111)-oriented terraces of the vicinal Rh(553) surface are virtually identical in terms of surface core-level shift energies. For very low CO exposures (0.05−0.1 L), the spectrum analysis indicates, however, that adsorption sites with a spectral signature at 285.65 eV BE (component T-s) are populated first. This component is ascribed to CO molecules adsorbed in on-top sites of Rh step atoms, on the basis of a calculated SCLS of −0.37 eV, i.e. to lower binding energy with respect to the T-t component, which is taken as a reference (see Table 2). This calculated value is in excellent agreement with the experimentally observed SCLS of −0.35 eV and also recent experiments of Resta et al.,[58] who found the respective T-s component at 285.7 eV BE. Thus, CO is adsorbed initially in on-top sites of Rh step atoms, but the on-top sites of Rh terrace atoms (T-t) follow closely in the sequence of population (see Figure 3b, spectra taken after 0.1 and 0.25 L CO exposures). Moreover, a further adsorption state is signaled in the spectra by an additional component at 285.25 eV BE, which arises after ∼0.25 L CO exposure. The DFT calculations yield an SCLS of −0.71 eV for CO adsorbed in two-fold bridge sites at steps (Br-s) and an SCLS of −0.65 eV for adsorption in the three-fold hollow sites at the step edge (H-s) in the limit of low coverages (Table 2). We therefore associate this spectral component, labeled Br(H)-s, with CO adsorbed in these higher-coordinated sites at the Rh steps. The sequence of the population of CO adsorption sites on Rh(553) as determined experimentally by C 1s HR-XPS spectra, recorded as a function of CO coverage, is therefore as follows: On-top sites at steps are occupied first, closely followed by on-top terrace sites; two-fold and hollow sites at steps are occupied next, and finally hollow terrace sites are filled.

TABLE 2: Experimental Values of the C 1s SCLS of CO on the Clean Rh(553) Surface and Theoretical Site Assignment Based on DFT Calculations

		core-level shift (eV)	
site	binding energy (eV)	expt	theory
T-t	286.00 ± 0.05	0	0
T-s	285.65 ± 0.05	−0.35	−0.37
Br-s	285.25 ± 0.05	−0.75	−0.71
H-s	285.25 ± 0.05	−0.75	−0.65
H-t	285.38 ± 0.05	−0.62	−0.61

Determining the activation energy for CO dissociation is more complicated for the stepped Rh surface than for the flat Rh

TABLE 3: Adsorption Energy (E), C−O Bond Length (d_{CO}), and C−X Distances (d_{C-X}, where X is the Metal Atom, for CO Adsorbed near and far from the Step Edge on Clean and Nickel-Decorated Rh(553) Surfaces[a]

	clean Rh(553)			Ni/Rh(553)		
site	E (eV)	d_{CO} (Å)	d_{C-X} (Å)	E (eV)	d_{CO} (Å)	d_{C-X} (Å)
			step			
top	−2.02	1.167	1.841(S)	−1.78	1.162	1.745(S)
br1	−2.05	1.187	1.990(S), 1.990(S)	−1.89	1.182	1.876(S), 1.876(S)
br2	−1.92	1.183	2.082(S), 2.070	−1.98	1.187	1.922(S), 1.965
fcc	−2.05	1.197	2.063(S), 2.063(S), 2.164	−2.09	1.198	1.981(S), 1.981(S), 2.034
hcp	−1.95	1.198	2.064(S), 2.100, 2.100	−2.12	1.199	1.975(S), 2.068, 2.068
			terr1			
top	−1.89	1.166	1.828	−1.91	1.166	1.827
br	−1.86	1.189	2.013, 2.013	−1.89	1.189	2.012, 2.012
fcc	−1.91	1.198	2.088, 2.088, 2.076	−1.96	1.198	2.088, 2.088, 2.086
hcp	−1.99	1.199	2.068, 2.085, 2.085	−2.01	1.200	2.080, 2.080, 2.080
			terr2			
top	−1.80	1.167	1.827	−1.84	1.167	1.827
br	−1.78	1.192	2.014, 2.014	−1.79	1.190	2.011, 2.011
fcc	−1.89	1.197	2.102, 2.102, 2.067	−1.91	1.197	2.099, 2.099, 2.073
hcp	−1.95	1.201	2.062, 2.088, 2.088	−1.98	1.201	2.066, 2.086, 2.086

[a] (S) indicates that d_{C-X} refers to the distance between C and the Rh (or Ni) atom directly at the step. step, terr1, and terr2 correspond to adsorption sites between the first and second atomic rows (step edge), between the second and third atomic rows, and between the third and fourth atomic rows on the upper terrace, respectively. For the step, br1 and br2 correspond to the bridge sites along the first atomic row and between the first and second atomic rows, respectively.

surfaces, mainly because of the diversity of molecular and atomic binding sites that exist on stepped surfaces. In our study, we focus exclusively on the investigation of the dissociation of a CO molecule at the step edge. We do not consider dissociation on the terraces, for which we expect results very similar to those obtained for the flat (111) surface. To the best of our knowledge, only a few previous theoretical studies were concerned with CO dissociation on a high-Miller-index Rh surface, specifically Rh(211).[54,55] The Rh(211) vicinal surface has a (100) microfacet, whereas the Rh(553) surface has a (111) microfacet. On the Rh(211) vicinal surface, the dissociation of CO takes place starting from the one-fold-coordinated state at the step.[55] In the final configuration, the C atom sits in the hollow site of the lower part of the step, and the oxygen atom has moved to the bridge position at the step. Although the local structure of the step and the morphology of the facet are different for the Rh(553) and Rh(211) surfaces, by analogy, we consider a reaction pathway similar to that for the Rh(211) surface.

In the lowest-energy TS, the C atom remains localized in the starting configuration, that is, the face-centered-cubic (fcc) hollow position at the lower terrace, and the oxygen atom migrates via the neighboring bridge site at the step edge (see Figure 2b). The results for the structural properties and activation energy are summarized in Table 1.

The reaction has an intrinsic dissociation barrier of +0.03 eV, i.e., slightly above the threshold for desorption. This value is significantly smaller than the activation barrier of 1.05 eV found on the flat Rh(111) surface. We note that the CO coverage used for the flat surface is higher than that used for the stepped surface, but in ref 59, it was shown that the dissociation barrier on Rh(111) does not depend to great extent on the coverage. Again, we find a rather late transition state. The CO distance is 2.033 Å, with the O atom sitting in a bridge position at the step with a distance of 1.970 Å; the C atom is near an fcc hollow position with the distances varying from 1.919 to 1.974 Å. We recall that, on the flat surface, the C atom is also sitting near a hollow position, and the O atom is near a bridge position, but they do not share any common metal atom at the stepped surface.

Experimentally, there is an ongoing debate whether CO dissociates on stepped Rh single-crystal surfaces. It has been demonstrated that the probability of CO dissociation on Rh(111) is negligible compared to the probability of molecular desorption.[60] On Rh(755) and Rh(331), partial CO dissociation has been reported during heating from 300 to 1000 K.[61] DeLouise and Winograd, in a comparative study of (111) and (331) Rh surfaces by X-ray photoelectron spectroscopy (XPS) and secondary-ion mass spectrometry (SIMS), however, failed to detect CO dissociation.[62] The densely packed Rh(111) [60,63,64] and (100)[65,66] surfaces were never found to be capable of breaking the C−O bond. On the other hand, it has been shown that CO dissociates on at least some more open surfaces such as Rh(210).[67]

If CO is first adsorbed at room temperature and the system is then heated, the ratio of dissociation to desorption (f_{diss}/f_{deso}) within transition state theory[55] is roughly given by ν_{diss}/ν_{deso} $\exp[-(E_{diss} - E_{deso})/kT]$,[55] where ν_{diss} and ν_{deso} are attempt frequencies in the rate expression for dissociation and desorption, respectively; $E_{diss} = E_{ts} - E_{ads}$; and $E_{deso} = -E_{ads}$. It follows that $E_{diss} - E_{deso} = E_{ts}$ By assuming similar prefactors within transition state theory ($\nu_{diss} \approx \nu_{deso}$) and using the calculated value of 1.05 eV for the flat surface, we have that f_{diss}/f_{deso} is extremely small at $T \approx 300$ K and, therefore, dissociation is very unlikely to occur on Rh(111). On the other hand, for the Rh(553) surface, we find a barrier of 0.03 eV, and therefore, some dissociation might be possible at room temperature or at elevated temperature.

We performed a very careful experimental search for indications of CO dissociation on Rh(553) using HR-XPS C 1s core-level spectroscopy. Our experimental results demonstrate that CO dissociation does not occur on Rh(553). In Figure 4a are displayed C 1s spectra of Rh(553) exposed to 0.5 and 20 L CO at 90 K and after the CO-covered surfaces had been heated to 520 K. The spectral profiles in the BE region of 285−287 eV are consistent with the spectra shown in Figure 3 at the respective CO coverages. Heating the CO-covered Rh(553) surfaces to 520 K leads to the desorption of CO molecules,[39] and the XPS spectra lose all intensity in the C 1s region.

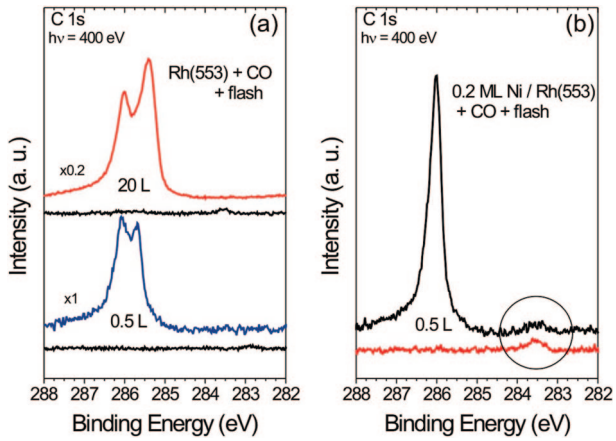

Figure 4. (a) XPS spectra of the C 1s binding energy region of Rh(553) exposed to 0.5 L of CO at 90 K and after this surface had been heated to 520 K. (b) Same as a for the 0.2 ML Ni-decorated Rh(553) surface. Notice the weak emission intensity at around 283.5 eV due to atomic carbon (circled).

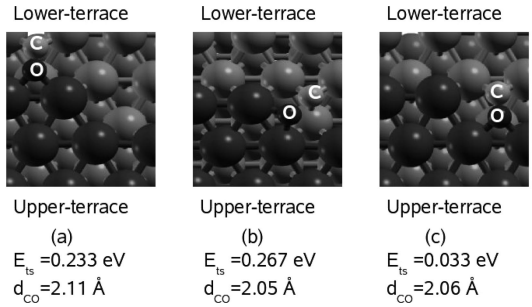

Figure 5. Top view of the TS geometry for CO dissociation at the kink sites of the clean Rh(553) surface. Pale gray spheres are Rh atoms; dark gray spheres are C and O atoms. a−c refer to different reaction paths at the kink (see text for details). Step atoms are labeled Rh.

Notably, there is no intensity at around 283−284 eV BE, which would indicate the presence of atomic carbon at the surface as a result of CO dissociation upon adsorption or during the desorption process. Thus, we detect no signs for dissociation of CO on the bare Rh(553) surface.

3.3. Kinks at the Stepped Rh(553) Surface. It is a common assumption that point defects such as kinks can be even more reactive than steps.[54,55] As kinks cannot be avoided experimentally, we explored the possibility of CO dissociation at a kink site at the step of the Rh(553) surface. For these calculations, the kinked surface was modeled as an asymmetric slab of four Rh layers parallel to the (111) terraces, with a p(4 × 1) unit cell containing four step atoms. The kinks were created by removing two step atoms. Each kink is characterized by two 120° corners, one convex and the other concave, giving rise to two steps with (111) and (100) microfacets (see Figure 5). Note that some atoms at the kink have an atomic coordination of six, that is, even lower than atoms at the stepped Rh(553) surface with no kinks.

Three different reaction paths were investigated: paths a and b are perpendicular to the triangular and square microfacets, respectively, in the convex part of the kink; path c is perpendicular to the triangular microfacet in the concave part of the kink (see Figure 5). The corresponding energy barriers and CO bond lengths are shown in Figure 5. The oxygen atom is at the bridge position, and the C atom is at the lower terrace hollow site in all three geometries. All of the transition states have a long stretched distance between C and O (late TSs). From Figure 5, we see that the dissociation barriers can vary by as much as 0.23 eV depending on the reaction path considered. Nevertheless, it is important to note that even the lowest TS still has an energy barrier of ∼0.03 eV, which is nearly the same as for the stepped Rh(553) surface without kinks (see Table 1). This suggests that CO dissociation does not occur at either the steps or the kinks of the Rh(553) surface.

4. Nickel-Decorated Rh(553) Surface

Step decoration is a useful method to vary the reactivity of the step sites in a local and controllable way. The properties of bimetallic Ni−Rh nanowires, fabricated by decorating the steps of vicinal Rh(111) surfaces by stripes of self-assembled Ni adatoms,[29] were already investigated in a previous publication.[68] It was found that these Ni−Rh nanowires have specific electronic properties that lead to a significantly enhanced chemical reactivity toward molecular oxygen. Therefore, it is interesting to probe the chemical reactivity of the nickel-decorated Rh(553) surface toward adsorption and dissociation of CO.

4.1. CO Adsorption at the Ni Steps and Terraces. In Table 3, we report the adsorption energies and structural parameters of CO adsorbed at the step and in neighboring terrace sites for the clean and nickel-decorated Rh(553). We note that the adsorption energies and bond lengths at the terrace (terr2) of the Ni-decorated surface are very similar to those for the clean Rh(553) surface, suggesting that the decoration of the step induces a very local effect with regard to CO adsorption. At the step edge, CO in low-coordinated sites (top and bridge) is bound more strongly on the clean Rh(553) surface than on the nickel-decorated one (the energy differences are up to 240 meV). On the other hand, CO in high-coordinated sites in the vicinity of the step edge is bound more strongly on the nickel-decorated surface than on the clean Rh(553) (the energies differences are up to 170 meV). This asymmetric behavior is most probably due to the different coordination of CO in low- and high-coordinated sites on the nickel-decorated and clean stepped surfaces. On the nickel-decorated surface, in a low-coordinated site, CO is bound to Ni atoms only; in a high-coordinated site, it is bound to two Ni and one Rh atoms for the fcc case and to one Ni and two Rh atoms for the hcp case. Obviously, on the clean Rh(553) surface, CO is bound to Rh atoms only. This indicates that an important role in the adsorption energy is played not only by the coordination to the metal atoms but also by the chemical type of the atoms coordinated with the adsorbed CO molecule. We see that, for the hcp site, the adsorption energy can vary by up to 170 meV with changes in the local atomic type of coordination. We note that, on the standard DFT (GGA) level, the most stable site at the step of the Rh(553) is the fcc site with an adsorption energy of −2.05 eV; on the nickel-decorated surface, the most stable site is hcp with an adsorption energy of −2.12 eV. The decoration of the step with nickel atoms thus stabilizes the most favored site by more than 50 meV. The picture changes slightly on a level beyond DFT. Reevaluating the energies with the HSE03 hybrid using the HSE03 functional, a general decrease of the adsorption strength in the vicinity of the step can be observed. For instance, the adsorption energies of the top, bridge, fcc, and hcp hollow site are −1.76, −1.95, −1.86, and −2.08 eV when evaluated using HSE03. Again, this effect is much stronger for molecules adsorbing directly at the Ni step edge than for adsorption at the Ni−Rh interface. The only exception is the adsorption at the hcp hollow site, which yields an HSE03 adsorption energy of −2.08 eV, comparable to that for the flat Rh(111) surface ($E_{ads(111)}$= −2.01 eV). Therefore, we predict that the adsorption

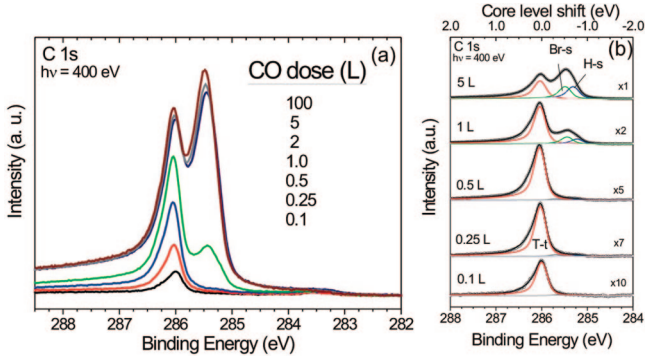

Figure 6. (a) C 1s XPS spectra of the 0.2 ML Ni-decorated Rh(553) surface after exposure to various amounts of CO at 90 K. (b) Quantitative decomposition analysis of selected C 1s spectra into different spectral components. For labeling, see text.

TABLE 4: Experimental Values of the C 1s SCLS of CO on the Ni/Rh(553) Surface and Theoretical Site Assignments Based on DFT Calculations

		core-level shift (eV)	
site	binding energy (eV)	expt	theory
T-t	286.00 ± 0.05	0	0
Br-s	285.45 ± 0.05	−0.55	−0.51
H-s	285.25 ± 0.05	−0.75	−0.70

of CO will rather start at the Rh(111) terrace and that adsorption at the Ni step edge will be suppressed.

Figure 6a shows a sequence of C 1s core-level spectra from the 0.2 ML Ni-decorated Rh(553) surface as a function of exposure to CO at 90 K. Selected spectra decomposed into various spectral components[56] are displayed in Figure 6b. It is noticed that, for low CO exposures, up to 0.5 L, the spectra exhibit a simple shape and only a single spectral component at 286.0 eV BE is necessary to fit the experimental data. This is quite different from the case on the clean Rh(553) surface (see Figure 3), for which three spectral components had to be included in the analysis of the data at these CO exposures. Significantly, there is no T-s component due to on-top sites at steps on the Ni-decorated Rh surface. On the basis of its binding energy at 286.0 eV, this component at the Ni-decorated surface is ascribed to CO molecules in on-top terrace sites (T-t). For higher CO exposures (>1 L), two additional spectral components become apparent in the data at BEs of 285.45 and 285.25 eV and grow roughly simultaneously in intensity with increasing CO exposure. The DFT calculations predict C 1s SCLSs of −0.51 and −0.70 eV for CO adsorbed in a Ni−Rh bridge site at the steps and a step hollow site, respectively (Table 4). We thus associate the spectral components at 285.45 and 285.25 eV with bridge step (Br-s) and hollow step (H-s) sites, repsectively. Note that, in this case, the bridge site correspond to the CO adsorption between the first and second atomic rows at the step, i.e., bri2 of Table 3.

Figure 7 shows a graph of the relative CO coverages at different adsorption sites, derived from the integrated intensities of the C 1s core-level components, as a function of the CO dose for the clean and Ni-decorated Rh(553) surfaces. The populations of the different adsorption sites by CO are noticeably different on the two surfaces. On clean Rh(553), the on-top sites at steps are slightly preferred over the on-top terrace sites, whereas the on-top terrace sites are clearly preferred on the Ni-decorated surface, and the occupation of higher-coordinated step sites (Br-s and H-s) follows at a significant delay. On-top step sites, that is, CO adsorption on top of Ni step atoms, have not

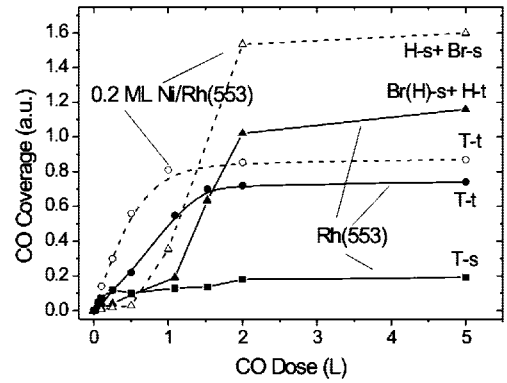

Figure 7. Plot of the relative coverage of CO at different adsorption sites versus CO dose, for clean Rh(553) (solid symbols) and for 0.2 ML Ni/Rh(553) (open symbols). T-s, on-top step site; T-t, on-top terrace site; H-s, hollow step site; H-t, hollow terrace site; Br-s, bridge step site.

been identified. Comparing the theoretical and experimental results, we find a consistent order of the low-coverage adsorption sites. The only discrepancy can be found in the assignment of the hcp hollow site at the Rh−Ni interface, which is predicted to be equally stable as the terrace top sites from the calculations, but is observed only at higher coverage. This difference can be attributed to the fact that even calculations at the HSE03 level do not necessarily include all aspects of the physics for the adsorption of CO.[69]

4.2. CO Dissociation at the Ni Steps. Finally, we investigate the effect of decoration of the step edges with nickel atoms on the dissociation of CO. The theoretical results are summarized in Table 1. The intrinsic dissociation barrier, E_{ts}, is −0.06 eV, significantly lower than for dissociation at the flat (111) surface (1.05 eV) and still lower than for dissociation at the clean stepped surface (0.03 eV). In particular, the change of sign in E_{ts} suggests that, upon heating, the adsorbed CO molecule would rather desorb on the clean Rh(553) surface (where E_{ts}, referred to the gas-phase zero, is positive), and that CO can dissociate on the nickel-decorated surface (where E_{ts} is negative). Although the low barrier of $E_{ts} = 0.03$ eV for the clean Rh(553) surface might allow for some dissociation at room temperature or at elevated temperatures, our experimental findings do not support this assumption.

The geometry of CO in the transition state is very similar to the configuration found on the clean Rh(553) surface: the C atom is in the fcc hollow site at the base of the step, with C−Rh distances slightly smaller (∼0.01 Å) than at the clean surface. This suggests that step decoration with different metal atoms does not change the overall TS geometry and that the reaction pathway can be transferred to different step-decorated surfaces. Significant differences were found for the distances between the oxygen atom and the nickel atoms at the step edge: they are 0.15 Å shorter, suggesting a stronger bonding between oxygen and nickel atoms. On the other hand, the CO bond in the TS complex is ∼0.05 Å longer.

The XPS experiments indicate that dissociation of CO on the Ni-decorated (553) surface does occur to a certain extent. Figure 4b displays the C 1s XPS spectra of the 0.2 ML Ni/Rh(553) surface after exposure to 0.5 L CO at 90 K and after flashing of the CO-covered surface to 520 K. Apart from spectral intensity in the BE region of 285−287 eV due to emission from the molecular CO, there is a weak emission intensity also at around 283.5 eV BE, which is characteristic of atomic carbon at the surface. The latter indicates that a small fraction of CO

might dissociate on Ni-decorated Rh(553), in agreement with the theoretical prediction. The majority of adsorbed CO still appears to desorb upon heating, but the balance of kinetic effects in the competition between desorption and dissociation might also be important.

5. Summary

We have performed a comparative study of carbon monoxide adsorption and dissociation on flat Rh(111), stepped Rh(553), and Ni-decorated Rh(553) surfaces using ab initio density functional theory and high-resolution XPS core-level measurements. A detailed analysis of the energy profile demonstrates that the dissociation barrier of CO is about 1 eV lower on the stepped Rh(553) surface than on the flat Rh(111) surface, but still above the desorption threshold. Including dissociation at the kink sites at the steps does not significantly change the results. Therefore, no dissociation of CO is predicted on the clean Rh(553) surface, in agreement with the experimental XPS measurements.

The chemistry can be significantly changed by decorating the step edge with metallic Ni stripes. In contrast to the behavior for the clean surface, the adsorption of CO starts not at the step edges, but rather at the flat terrace. The barrier for the dissociation of CO at the Ni wires is about 0.1 eV lower than that on the clean Rh(553) surface, allowing for a partial dissociation of CO. Therefore, it might be possible to tune the barriers for dissociation with an appropriate choice of step decoration and, at the same time, to control the poisoning by the local modification of the adsorption strength. This possibility will be investigated in a forthcoming publication.

Acknowledgment. This work was supported by the Austrian Research Funds through the National Research Network "Nanoscience on Surfaces". The experiments at the MAX-Laboratory synchrotron radiation laboratory were supported by the EU TMR Programme. F.P.N. acknowledges with gratitude the excellent hospitality of Prof. W.-D. Schneider during his sabbatical stay at the Institut de Physique des Nanostructures, EPFL, Lausanne, Switzerland. A.S. thanks T. Bucko for kind assistance with the dimer calculations.

References and Notes

(1) Blyholder, G. *J. Phys. Chem.* **1964**, *68*, 2772.
(2) Bagus, P. S.; Nelin, C. J.; Bauschlicher, C. W. *Phys. Rev. B* **1983**, *28*, 5423.
(3) Davis, S. M.; Somorjai, G. A. In *The Chemical Physics of Solid Surfaces*; King, D. A., Woodruff, D. A., Eds.; Elsevier: Amsterdam, 1982; Vol. 4.
(4) Sung, S.; Hoffmann, R. *J. Am. Chem. Soc.* **1985**, *107*, 578.
(5) Over, H. *Prog. Surf. Sci.* **2001**, *58*, 249.
(6) Henry, C. R. *Surf. Sci. Rep.* **1998**, *31*, 231.
(7) Campazona, J. C. In *The Chemical Properties of Solid Surfaces and Heterogenous Catalysis*; King, D. A., Woodruff, D. P., Eds.; Elsevier: Amsterdam, 1990; Vol. 3, Part A.
(8) Wagner, H. In *Springer Tracts in Modern Physics*; Hoehler, G., Ed.; Springer: Berlin, 1987.
(9) Curulla, D.; Linke, R.; Clotet, A.; Ricart, J. M.; Niemantsverdriet, J. W. *Chem. Phys. Lett.* **2002**, *354*, 503.
(10) Linke, R.; Curulla, D.; Hopstaken, M. J. P.; Niemantsverdriet, J. W. *J. Chem. Phys.* **2001**, *115*, 8209.
(11) Beutler, A.; Lundgren, E.; Nyholm, R.; Andersen, J. N.; Setlik, B.; Heskett, D. *Surf. Sci.* **1997**, *371*, 381.
(12) Beutler, A.; Lundgren, E.; Nyholm, R.; Andersen, J. N.; Setlik, B.; Heskett, D *Surf. Sci.* **1998**, *396*, 117.
(13) Gierer, M.; Barbieri, A.; van Hove, M. A.; Somorjai, G. A. *Surf. Sci.* **1997**, *391*, 176.
(14) Lundgren, E.; Torrelles, X.; Alvarez, J.; Ferrer, S.; Over, H.; Beutler, A.; Andersen, J. N. *Phys. Rev. B* **1999**, *59*, 5876.
(15) Wie, D. H.; Skelton, D. C.; Kevan, S. D. *Surf. Sci.* **1997**, *381*, 49.
(16) Smedh, M.; Beutler, A.; Ramsvik, T.; Nyholm, R.; Borg, M.; Andersen, J. N.; Duschek, R.; Sock, M.; Netzer, F. P.; Ramsey, M. G. *Surf. Sci.* **2001**, *491*, 99.
(17) Vannice, M. A. *J. Catal.* **1975**, *37*, 449.
(18) Ichikawa, M. *Bull. Chem. Soc. Jpn.* **1978**, *51*, 2268.
(19) Bhasin, M. M.; Bartley, W. J.; Ellgen, P. C.; Wilson, T. P. *J. Catal.* **1978**, *120*, 54.
(20) For a review, see: Wandelt, K. *Surf. Sci.* **1991**, *251/252*, 3871.
(21) Hammer, B.; Norskov, J. K. *Adv. Catal.* **2000**, *45*, 71.
(22) Hammer, B. *Surf. Sci.* **2000**, *459*, 323.
(23) Hammer, B. *Top. Catal.* **2006**, *37*, 3.
(24) Gambardella, P.; Blanc, M.; Kuhnke, K.; Kern, K.; Picaud, F.; Ramseyer, C.; Girardet, C.; Barreteau, C.; Spanjaard, D.; Desjonquères, M. *Phys. Rev. B* **2001**, *64*, 45404.
(25) Hammer, B. *Phys. Rev. Lett.* **1999**, *83*, 3681.
(26) Zambelli, T.; Wintterlin, J.; Trost, J.; Ertl, G. *Science* **1996**, *273*, 1688.
(27) Shen, J.; Klaua, M.; Ohresser, P.; Jenniches, H.; Arthel, J. B.; Mohan, C. V.; Kirschner, J. *Phys. Rev. B* **1997**, *56*, 11134.
(28) Gambardella, P.; Blanck, M.; Brune, H.; Kuhnke, K.; Kern, K. *Phys. Rev. B* **2000**, *61*, 2554.
(29) Schoiswohl, J.; Mittendorfer, F.; Surnev, S.; Ramsey, M. G.; Andersen, J. N.; Netzer, F. P. *Surf. Sci.* **2006**, *600*, L274.
(30) Hammer, B.; Hansen, L. B.; Norskov, J. K. *Phys. Rev. B* **1999**, *59*, 7413.
(31) Gajdos, M.; Eichler, A.; Hafner, J. *J. Phys.: Condens. Matter* **2004**, *16*, 1141.
(32) Stroppa, A.; Termentzidis, K.; Paier, J.; Kresse, G.; Hafner, J. *Phys. Rev. B* **2007**, *76*, 195440.
(33) Yates, J. T., Jr.; Williams, E. D.; Weinberg, W. H. *Surf. Sci.* **1980**, *1*, 562.
(34) Ren, D. M.; Liu, W. *Surf. Sci.* **1990**, *232*, 316.
(35) Rebholz, M.; Prins, R.; Kruse, N. *Surf. Sci.* **1991**, *259*, L797, and references therein.
(36) Frank, M.; Andersson, S.; Libuda, J.; Stempel, S.; Sandell, A.; Brena, B.; Giertz, A.; Brühwiler, P. A.; Bäumer, M.; Martensson, N.; Freund, H.-J. *Chem. Phys. Lett.* **1997**, *279*, 92; *Chem. Phys. Lett.* **1999**, *310*, 229.
(37) Andersson, S.; Frank, M.; Sandell, A.; Giertz, A.; Brena, B.; Bruhwiler, P. A.; Martensson, N.; Libuda, J.; Bäumer, M.; Freund, H.-J. *J. Chem. Phys.* **1998**, *108*, 2967.
(38) Ertl, G.; Freund, H.-J. *Phys. Today* **1999**, *52*, 32.
(39) Koch, H. P.; Singnurkar, P.; Schennach, R.; Stroppa, A.; Mittendorfer, F. *J. Phys. Chem. C* **2008**, *112*, 806.
(40) Kresse, G.; Hafner, J. *Phys. Rev. B* **1993**, *47*, C558.
(41) Kresse, G.; Furthmuller, J. *Comput. Mater. Sci.* **1996**, *6*, 15.
(42) Perdew, J. P.; Burke, K.; Ernzerhof, M. *Phys. Rev. Lett.* **1996**, *77*, 3865.
(43) Heyd, J.; Scuseria, G. E.; Ernzerhof, M *J. Chem. Phys.* **2003**, *118*, 8207.
(44) Blöchl, P. E. *Phys. Rev. B* **1994**, *50*, 17–953.
(45) Kresse, G.; Joubert, D. *Phys. Rev. B* **1999**, *59*, 1758.
(46) Mantz, A. W.; Watson, J. K. G.; Rao, K. N.; Albritton, D. L.; Schmeltekope, A. L.; Zare, R. N. *J. Mol. Spectrosc.* **1971**, *39*, 180.
(47) Mills, G.; Jonsson, H. *Phys. Rev. Lett.* **1994**, *72*, 1124.
(48) Mills, G.; Jonsson, H.; Schenter, G. K. *Surf. Sci.* **1995**, *324*, 305.
(49) Jonsson, H.; Mills, G.; Jacobsen, K. W. In *Classical Quantum Dynamics in Condensed Phase Simulations*; Berne, B. J., Ciccotti, G., Coker, D. F., Eds.; World Scientific: Singapore, 1998; p 385.
(50) Heyden, A.; Bell, A. T.; Keil, F. J. *J. Chem. Phys.* **2005**, *123*, 224101.
(51) Henkelman, G.; Jónsson, H. *J. Chem. Phys.* **1999**, *111*, 7010.
(52) Köhler, L.; Kresse, G. *Phys. Rev. B* **2004**, *70*, 165405.
(53) Nyholm, R.; Andersen, J. N.; Johansson, U.; Jensen, B. N.; Lindau, I. *Nucl. Instrum. Methods Phys. Res.* **2001**, *A467−468*, 320.
(54) Liu, Z.-P.; Hu, P. *J. Chem. Phys.* **2001**, *114*, 8244.
(55) Mavrikakis, M.; Bäumer, M.; Freund, H.-J.; Norskov, J. K. *Catal. Lett.* **2002**, *81*, 153.
(56) Each of the core-level components in the C 1s peak decomposion analysis was coupled to vibrational satellites (not shown for clarity), with relative intensity and position with respect to the main adiabatic peaks as established for different CO adsorption geometries on Rh(111). See: Smedh, M.; Beutler, A.; Ramsvik, T.; Nyholm, R.; Borg, M.; Andersen, J. N.; Duschek, R.; Sock, M.; Netzer, F. P.; Ramsey, M. G. *Surf. Sci.* **2001**, *491*, 99.
(57) Beutler, A.; Lundgren, E.; Nyholm, R.; Andersen, J. N.; Setlik, B. J.; Hesket, D. *Surf. Sci.* **1998**, *396*, 117.
(58) Resta, A.; Lundgren, E.; Mikkelsen, A.; Gustafson, J.; Wang, J. G.; Hammer, B.; Andersen, J. N. *MAX-Lab Activity Report*; Lund University: Lund, Sweden, 2005−2006; p 178
(59) Liu, Z. P.; Hu, P. *J. Am. Chem. Soc.* **2003**, *125*, 1958.
(60) Yates, J. T., Jr.; Williams, E. D.; Weinberg, W. H. *Surf. Sci.* **1980**, *91*, 562.
(61) Castner, D. G.; Somorjai, G. A. *Surf. Sci.* **1979**, *83*, 60.

(62) DeLouise, L. A.; Winograd, N. *Surf. Sci.* **1984**, *138*, 417.
(63) Castner, D. G.; Sexton, B. A.; Somorjai, G. A. *Surf. Sci.* **1978**, *71*, 519.
(64) Thiel, P. A.; Williams, E. D.; Yates, J. T., Jr.; Weinberg, W. H. *Surf. Sci.* **1979**, *84*, 54.
(65) Kim, Y.; Peebles, H. C.; White, J. M. *Surf. Sci.* **1982**, *114*, 363.
(66) Gurney, B. A.; Richter, L. J.; Villarubia, J. S.; Ho, W. *J. Chem. Phys.* **1987**, *87*, 6710.
(67) Rebholz, M.; Prins, R.; Kruse, N. *Surf. Sci. Lett.* **1991**, *259*, L797.
(68) Schoiswohl, J.; Mittendorfer, F.; Surnev, S.; Ramsey, M. G.; Andersen, J. N.; Netzer, F. P. *Phys. Rev. Lett.* **2006**, *97*, 126102.
(69) Stroppa, A.; Kresse, G. *New J. Phys.* **2008**, *10*, 063020.

JP806424T